Biosensors and Bioelectronics 35 (2012) 160–166

Contents lists available at SciVerse ScienceDirect

Biosensors and Bioelectronics

journal homepage: www.elsevier.com/locate/bios

A novel approach to determining the affinity of protein–carbohydrate interactions employing adherent cancer cells grown on a biosensor surface

Diluka Peiris, Anatoliy Markiv, G. Paul Curley, Miriam V. Dwek*

Department of Molecular and Applied Biosciences, School of Life Sciences, University of Westminster, 115 New Cavendish St., London W1W 6UW, England, UK

ARTICLE INFO

Article history:
Received 12 December 2011
Received in revised form 15 February 2012
Accepted 17 February 2012
Available online 25 February 2012

Keywords:
Biosensor
Lectin
Affinity
Dissociation constant
Quartz crystal microbalance (QCM)
Surface plasmon resonance (SPR)
Recombinant protein
Helix pomatia agglutinin (HPA)

ABSTRACT

The development of biological agents for the treatment of solid tumours is an area of considerable activity. We are pursuing carbohydrate-binding proteins (lectins) in a strategy aimed at targeting cancer-associated changes in glycosylation. To evaluate lectin–cancer cell interactions we developed a novel cell biosensor in which binding events take place at the cell surface, more closely mimicking an *in vivo* system. Metastatic, SW620, and non-metastatic, SW480, colorectal cancer cells were grown on the surface of a tissue-culture compatible polystyrene coated biosensor chip and housed in a quartz crystal microbalance (QCM) apparatus, the kinetics of binding of a diverse range of lectins was evaluated. The lectin *Helix pomatia* agglutinin (HPA) has been shown to bind aggressive metastatic cancer and was produced in recombinant form (His- and RFP-tagged). The affinity of HPA was in the nanomolar range to the metastatic SW620 cells but was only in the micromolar range to the non-metastatic SW480. Overall, the dissociation constant (K_D) of the lectins tested in the new cell biosensor system was an order of magnitude lower (nanomolar range) than has generally been reported with systems such as QCM/SPR. This new cell-biosensor enables molecular interactions to be studied in a more relevant environment. An intrinsic problem with developing new biological therapies is the difficulty in determining the affinity with which proteins will interact with intact cell surfaces. This methodology will be of interest to researchers developing new biological approaches for targeting cell surfaces in a wide range of diseases, including cancer.

1. Introduction

The development of pharmaceuticals is a costly enterprise with a significant attrition rate in the pre-clinical testing phase. New techniques are needed to provide information on the possible *in vivo* properties of novel biotherapeutics. A key step in the drug-development pipeline is evaluation of the affinity (dissociation constant, K_D) of the new biotherapeutic to its epitope. This is determined by measuring the on- and off-rate of the biotherapeutic to purified ligand immobilised (often *via* a spacer-molecule) to a planar surface. Unfortunately, however, this approach does not take into consideration the *in vivo* presentation of ligand. In the case of cell surface ligands these are found on the cell membrane in a milieu that includes diverse molecules in clusters, calthrin-coated pits, transmembrane proteins, lipids, GPI-anchored proteins and carbohydrates – all of which might potentially interfere with an interaction between a biotherapeutic and its ligand. We developed a system to assess the affinity of carbohydrate-binding proteins (lectins) to glycans directly at the cell surface and compared this with glycoproteins that had been immobilised on a planar surface.

The new biosensor system is based on the quartz crystal microbalance (QCM) technology and utilised adherent (tumour) cells grown on the surface of a gold sensor chip pre-coated with tissue culture compatible polystyrene. In the present study cancer cells were grown on the chip surface and were fixed in formaldehyde, the fixation process enabled regeneration of the cell surface between each interaction study and the cell chip to be used repeatedly, for approximately 20–30 experiments. Fixation in formaldehyde cross-links glycoproteins (Nirmalan et al., 2008), therefore, the formaldehyde fixation process might render some glycan epitopes less-accessible and reduce lectin binding but this is not considered to alter the overall binding pattern to cell surfaces (Brooks et al., 1998). Regeneration of non-fixed cells is a problem so we have worked on formalin-fixed cells as these cells represent a new model for the study of drug interactions at the cell surface. The system allows the study of interactions in the presence of other proteins that are normally found at the cell surface in contrast with conventional work using planar systems where, usually, simple, single protein/glycan entities are investigated. The applicability of the system is demonstrated with cancer cells and lectins although we consider the method to be of value for the

* Corresponding author. Tel.: +44 020 7911 5000x64158; fax: +44 020 7911 5086.
E-mail address: m.v.dwek@westminster.ac.uk (M.V. Dwek).

0956-5663/$ – see front matter.
doi:10.1016/j.bios.2012.02.037

evaluation of antibody–antigen and receptor–ligand interactions, and hope that this system is of interest to researchers working in diverse areas concerned with drug-development.

The QCM technique measures a change in resonance frequency (ΔF) as a mass accumulates on a quartz crystal (Sauerbrey, 1959), it is a label-free technique for studying biological interactions in real-time (Marx, 2003). Applications include off-rate screening, affinity measurement, epitope mapping and analysis of the thermodynamics of interactions, the technology has shown versatility and broad applicability for the analysis of molecular interactions (Pei et al., 2005; Cooper and Singleton, 2007; Pedroso et al., 2008; D'Ulivo et al., 2010; Johansson, 2010).

Previous studies have employed glycoconjugates immobilised onto sensor surfaces by amine coupling, physiosorption or by capture, for example, with streptavidin (Pei et al., 2005; Pedroso et al., 2008; Yakovleva et al., 2010). The analyte is typically injected over the sensor surface and changes in resonance frequency (ΔF) is monitored. The spatial arrangement of ligands at the sensor surface and concomitant binding has been the subject of a number of studies, for example by employing polymers in relation to enzyme binding properties (Marx et al., 2001).

Other recent studies have been concerned with measuring the kinetics of interaction between proteins and cell surfaces. These studies have often used a cell suspension and commonly trap the cells onto the sensor surface, by, for example, pre-coating the sensor with streptavidin and biotinylating the cells (Kuo et al., 2011), or by coating the surface of a biosensor with an antibody to facilitate the capture of cells on the surface (Saitakis et al., 2008). An issue with this approach, however, is that whilst being relatively fast and easy, it is best suited to cells that either grow as suspension cultures; or that are tolerant of being prepared as a cell suspension and is also dependent upon the method of cell capture. It is therefore of limited applicability for the analysis of cells that routinely grow as mono-layer culture and from a cell biology perspective it is desirable that methods be developed in which cells are grown as mono-layers prior to undertaking studies aimed at measuring cellular interactions. In an approach towards studying the entire cell surface, in a biosensor chip set-up, have shown that adherent cells may be grown and maintained on a gold sensor surface "treated chemically to render it hydrophilic" in a study concerned with microtubule arrangement and the effect of taxol and nocodazole treatment, however, the study did not address the interaction of biomolecules at the cell surface. Other reports have been concerned with the appropriate conditions for cell attachment and spreading (Modin et al., 2006; Fredriksson et al., 1998). The approaches that have used live cells in biosensor applications are not concerned with protein–cell interactions; rather they tend to focus on aspects of cell biology, for example cell adhesion and intracellular microtubule assembly. A recent review of this area shows the diverse approaches that have been taken to evaluate QCM sensors as tools for studying whole-cell interactions (Saitakis and Gizeli, 2012).

The applicability of the QCM-cell sensor system is shown here using a range of lectins including a recombinant form of the lectin: *Helix pomatia* agglutinin, HPA (Markiv et al., 2011) this is being developed in our laboratories as a tool for cancer prognostication and is also being pursued in a strategy aimed at biological targeting of cancer cells. Recombinant HPA was prepared either with a His-tag or a red fluorescent protein tag, and the binding properties to cancer cell membranes were compared with that of native HPA.

The method described here is suitable for investigations using a wide-range of biological systems and is an approach for measuring the kinetics of binding at the cell surface. We expect that the system will be of considerable interest to researchers targeting cell surface interactions with biological reagents as well as those developing the next generation of therapeutic antibodies.

2. Materials and methods

Chemicals were obtained from Sigma–Aldrich, Poole, Dorset, UK, unless otherwise stated. HPA lectin was purchased from Sigma–Aldrich and all other lectins were purchased from Vector laboratories, UK. All experiments were undertaken at 20 °C unless otherwise stated.

2.1. SW620 and SW480 cell culture

The human colorectal cancer cell lines SW620 (derived from mesenteric lymph node metastases) and SW480 (derived from Duke's B primary tumour of the colon of the same patient as the SW620 cells) were grown in Dulbecco's Modified Eagle's Medium (DMEM) (Lonza, UK) supplemented with 10% (v/v) foetal calf serum (Biosera). SW620 cells have been shown to exhibit a metastatic phenotype when implanted subcutaneously into SCID mice whilst SW480 cells are non metastatic (Schumacher et al., 1996; Schumacher and Adam, 1997). Cells were kindly provided by Dr Loizidou (Royal Free and University College London). Cells were cultured using standard tissue culture techniques. Cells used for protein extraction were grown to 90–95% confluence, washed in PBS, mechanically detached in PBS using a sterile plastic cell scraper and centrifuged at 400 × *g* and were stored at −80 °C prior to protein extraction. Cell membrane proteins were prepared from the SW620 and SW40 as we aimed to compare the kinetics of lectin binding to the proteins with the kinetics of lectin binding to intact cells grown on the sensor surface. Cell pellets were re-suspended in lysis buffer (7 M urea, 4% (w/v) CHAPS, 1% (w/v) DTT, 2% (v/v) ampholytes and 2 M thiourea) and lysed by sonication using an ultrasonic probe (MS73 Status 200) at 40% power (Philip Harris Scientific, UK), with 5 pulses of 10 s each. Cellular debris was removed by centrifugation, using a Sorvall Super T21 centrifuge with a SL50T rotor, for 30 min at 11,000 × *g*, 4 °C and cell membrane proteins were prepared by ultracentrifugation (Lehner et al., 2003).

2.2. Preparation of cell-biosensor chips

Cells were grown on the chips and fixed in formaldehyde prior to evaluation in the biosensor. Cell culture compatible polystyrene coated QCM sensor chips were obtained from Attana AB (Stockholm, Sweden). The sensor chip was placed, face-up, in a well of a 24-well plate. An appropriate dilution of cells (to obtain 40,000 cells on the sensor surface) was added in 2 ml of media to the well and the plate was placed in an incubator at 37 °C (5% (v/v) CO_2 and 95% humidity) for 20 h. Following incubation, the cells were washed 3× with PBS and fixed for 30 min in fresh 3.7% (v/v) formaldehyde in PBS. To evaluate the cell coverage the nuclei were stained with To-Pro-3 and visualised using a confocal microscope (Saint-Guirons et al., 2007). For each cell type, two separate passages of cells were assessed. The QCM analysis was undertaken using a range of lectins, at different concentrations, each time in triplicate.

2.3. Preparation of protein-biosensor chips

Biosensor chips containing cell membrane proteins were prepared to compare with the cell chips (above). Polystyrene chips (Attana AB, Stockholm, Sweden) were fitted to the chip holder, pre-wetted by manual injection of 20 μl of 10 mM sodium acetate buffer, pH 5.0. 20 μl of cell membrane protein preparation (250 μg/ml) was injected into the chamber, wrapped in Parafilm and incubated for 3 h at room temperature and the chip was inserted into the QCM machine as described below. For each protein preparation, two separate passages of cells were assessed. The

Table 1
The lectins used in this study and their principal binding partners. The association rate constant (k_{on}) and the dissociation rate constant (K_D) values were derived ($n = 2$) ± SE for lectins WGA, ConA, SJA, PHA-E, RCA, UEA-1, and HPA using the metastatic (SW620) and non-metastatic cells (SW480). No interaction was detectable with SJA when either SW620 or SW480 cells were evaluated using this lectin. The binding partners are D-Glc*p*N, D-Gal*p*N, Neu, αD-Man, D-Gal and L-Fuc.

Lectin	Binding partner	Association rate constant (k_{on}, M^{-1} s^{-1})		Dissociation constant (K_D, nM)	
		SW620 cells	SW480 cells	SW620 cells	SW480 cells
Triticum vulgaris, wheat germ agglutinin (WGA)	βD-Glc*p*N (1→4) Neu	$2.04 \times 10^4 \pm 820$	$1.42 \times 10^5 \pm 37{,}500$	370 ± 10	32.1 ± 3.0
Canavalia ensiformis, Concanvalin A, Jack bean (ConA)	αD-Man, complex N-glycans	$6.13 \times 10^3 \pm 240$	$3.32 \times 10^3 \pm 480$	33.7 ± 3.0	95.6 ± 1.0
Phaseolus vulgaris erythroagglutinin, common bean (PHA-E)	D-Gal bisected complex N-glycans	$7.59 \times 10^4 \pm 4300$	$4.98 \times 10^3 \pm 760$	34.4 ± 2.0	23.7 ± 2.0
Ricinus communis agglutinin, castor oil lectin (RCA)	D-Gal > D-Gal*p*N	$8.7 \times 10^4 \pm 6200$	$4.2 \times 10^4 \pm 3140$	64.7 ± 2.0	52.4 ± 10
Ulex europaeus agglutinin-1, gorse (UEA-1)	αL-Fuc (1 → 2)	$1.64 \times 10^4 \pm 2300$	$1.22 \times 10^2 \pm 14$	745 ± 30	$2.37 \times 10^4 \pm 1280$
H. pomatia agglutinin, Roman snail (HPA)	αD-Gal*p*N	$3.21 \times 10^4 \pm 5300$	$7.99 \times 10^3 \pm 570$	118 ± 40	$9.80 \times 10^5 \pm 4300$
Sophora japonica agglutinin, Japanese Pagoda tree (SJA)	βD-Gal*p*N	–		–	–

QCM analysis was undertaken using a range of lectins, at different concentrations, each time in triplicate.

2.4. Quartz crystal microbalance (QCM) analysis

All experiments were performed using an Attana Cell 100 or Attana Cell 200 biosensor (Attana AB, Stockholm, Sweden). The running buffer was PBS with 0.025% (v/v) Tween-20 for cells and PBS, with 0.05% (w/v) BSA and 0.025% (v/v) Tween-20 for protein chips. Chips were fitted to the machine and allowed to stabilise overnight at 20 °C at a flow rate of 25 μl/min. Lectins were injected over the surface of the chips at a range of concentrations, allowed to bind for 85 s and the dissociation was followed for 165 s. Following each association and dissociation cycle, the cell chip was regenerated using two 30 s pulses of 10 mM glycine, pH 1.0, 0.5 M NaCl, and immediately re-equilibrated with running buffer. The binding properties of a range of diverse plant lectins (Table 1) and also native HPA and recombinant HPA (see below) was evaluated using SW620 and SW480 cells as well as the cell membrane proteins, from SW620, prepared and immobilised on polystyrene chips. Lectins were injected at 79 nM, 159 nM, 316 nM and 632 nM. The surface was regenerated between each binding event as described above. The association/dissociation phases were monitored using the Attester software (Attana AB, Sweden). The software system used in the Attana apparatus presents the read-out from the detector as the $-\Delta F$ value. The kinetic parameters were determined using a simple 1:1 model compensated for mass-transport limitation (Evaluation software, Attana AB, Sweden), according to the following reaction.

$$A_0 \underset{k_m}{\overset{k_m}{\rightleftarrows}} A$$

$$A + B \underset{k_b}{\overset{k_a}{\rightleftarrows}} AB$$

where A is an analyte, B is an immobilised ligand and AB is the complex formed. The association (k_a) and dissociation (k_d) rate constants are determined. From these values the dissociation constant (K_D) and association constant (K_A) are calculated as follows: $K_D = 1/K_A = k_d/k_a$. The mass-transport coefficient (k_m) accounts for mass-transport-limited diffusion of the injected molecule between the bulk flow ($A0$) and the sensor surface (A).

2.5. Preparation of recombinant HPA

Recombinant HPA was prepared (Markiv et al., 2011) using a pET32a expression vector system (Supplementary data 1). An *in silico* structure of HPA-RFP and native HPA was modelled using SwissModel, an automated protein modelling server (Schwede et al., 2003) based on the structure of HPA (PDB accession number: 2CCV) (Sanchez et al., 2006) and RFP (PDB accession number: 2QLG). The resulting models were optimised using the MiFit software (version 3.0.1), Rigaku Corporation, Japan and visualised using the PyMol molecular graphic system.

2.6. Inhibition of HPA binding using 2-(Acetylamino)-2-deoxy-D-galactose (GalNAc)

The specificity of HPA binding to SW620 cells was evaluated by pre-incubating the lectin for 30 min in freshly prepared running buffer containing GalNAc (0.01–0.23 mM), this step was undertaken to ensure that all the binding sites were occupied. This HPA–GalNAc mixture was then injected over the cell chip and the association/dissociation phases were monitored. An appropriate concentration of GalNAc, without HPA, was injected prior to each measurement and was subtracted from the association curve as a blank. The maximal frequency shift monitored at the end of the association phase (after referencing with the GalNAc-containing solution) was used to calculate the binding of HPA at each GalNAc concentration.

2.7. Confocal microscopy

We compared the association rate constant (k_{on}, on-rate) for lectins to the cells (cell-chip biosensor data) with the overall lectin binding as assessed using cytochemistry and confocal microscopy (Saint-Guirons et al., 2007). Briefly, cells were prepared in 6-well plates, fixed in formaldehyde, blocked with BSA, incubated with TRITC- or FITC-labelled lectins (0.063 mM) for 1 h and counter-stained with 1 mM To-Pro-3. Images were acquired by sequential scanning using a Leica TCS SP2 confocal system (Leica

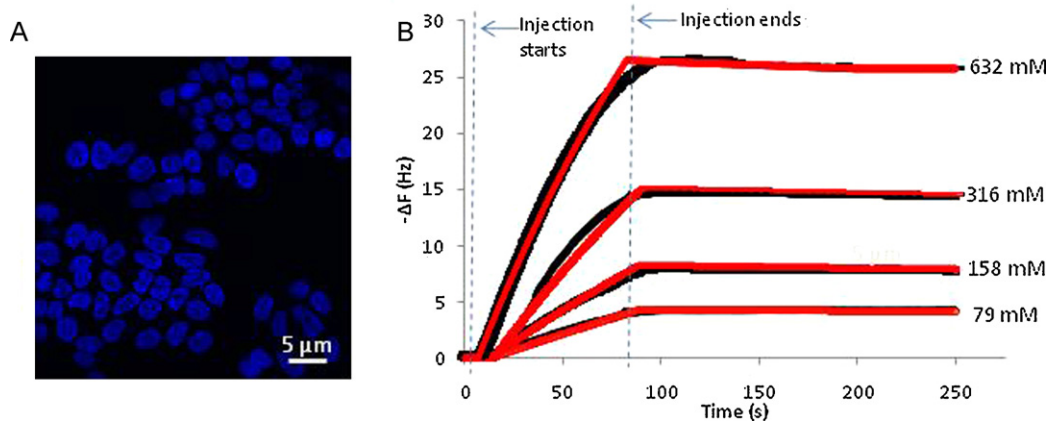

Fig. 1. Experimental design for the biosensor analysis. Panel A: SW620 cells grown on the sensor surface prior to inserting into the Attana Cell 200, nuclei are visible following staining with 1 mM To-Pro3 (Blue); Panel B: binding of lectin HPA-RFP to SW620 cancer cells. The sensorgrams show binding of the lectin at different concentrations (black) overlaid with theoretical curves generated using the mass transport model (red). (For interpretation of the references to colour in this figure legend, the reader is referred to the web version of this article.)

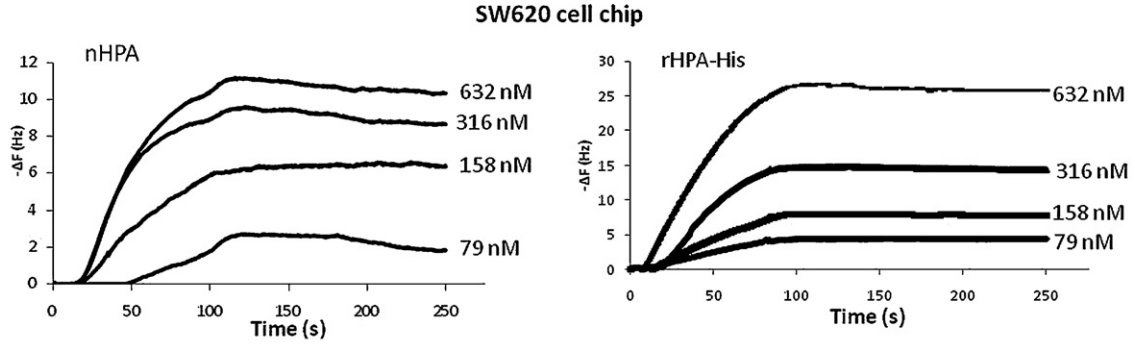

	SW620 cells			SW620 membrane proteins		
	k_{on} ($M^{-1}s^{-1}$)	k_{off} (s^{-1})	K_D (nM)	k_{on} ($M^{-1}s^{-1}$)	k_{off} (s^{-1})	K_D (nM)
nHPA	$3.21 \times 10^4 \pm 5.3 \times 10^3$	$3.79 \times 10^{-3} \pm 8.3 \times 10^{-4}$	118 ± 40	$7.99 \times 10^3 \pm 5.9 \times 10^2$	$6.867 \times 10^{-3} \pm 5.6 \times 10^{-4}$	859 ± 122
rHPA -His	$3.73 \times 10^4 \pm 2.8 \times 10^3$	$2.53 \times 10^{-4} \pm 2.7 \times 10^{-5}$	8.84 ± 0.9	$1.25 \times 10^4 \pm 1.8 \times 10^3$	$9.06 \times 10^{-3} \pm 1.9 \times 10^{-4}$	724+78
rHPA-RFP	$3.53 \times 10^4 \pm 4.7 \times 10^3$	$2.74 \times 10^{-4} \pm 1.8 \times 10^{-5}$	7.18 ± 0.7	-	-	-

Fig. 2. Sensorgrams illustrating the binding of native HPA (nHPA) and recombinant HPA-His (rHPA-His) onto SW620 cells grown on the chip surface. The association (85 s) and dissociation (165 s) phases were monitored for HPA at a range of concentrations as shown. The flow rate was maintained at 25 µl/min and the temperature was 20 °C. Mean average values ± SD, derived from the Evaluation software system (Attana, AB) are shown in the table.

Microsystems, Milton Keynes, UK) with a 63× ceramic dipping objective. A 488 nm laser was used for excitation of FITC, while a 543 nm laser was used for TRITC excitation. A 633 nm laser, intensity 35%, was used for To-Pro-3. The images from the green/red channel were overlaid with the image from the blue channel using the Imaris software system, version 7 from Bitplane.

2.8. Statistical analysis

For the QCM work the k_{on} and k_{off} values were measured for two biological and three analytical repeats, giving $n = 6$. The mean average value and the standard deviation were calculated for each condition tested. For the confocal microscopy, three low-power fields were captured and a representative field is shown for each of the lectins tested.

3. Results and discussion

Adherent cells were grown on a QCM biosensor chip surface and the affinity of interaction between cells and lectins was assessed. The system utilised human colorectal cancer cells derived from a primary cancer, SW480, and cells from metastases of the same patient, SW620. Whilst the applicability of the QCM technology for monitoring real-time binding of lectins with carbohydrates has previously been evaluated with immobilised lectins (Barnes et al., 1992; Pedroso et al., 2008; Safina et al., 2011; Yakovleva et al., 2010) and carbohydrates (Pei et al., 2005), to our knowledge this is the first report in which cells have been grown directly on the sensor surface and used to study lectin–carbohydrate interactions. Fig. 1 illustrates the experimental design and the strategy for the data analysis.

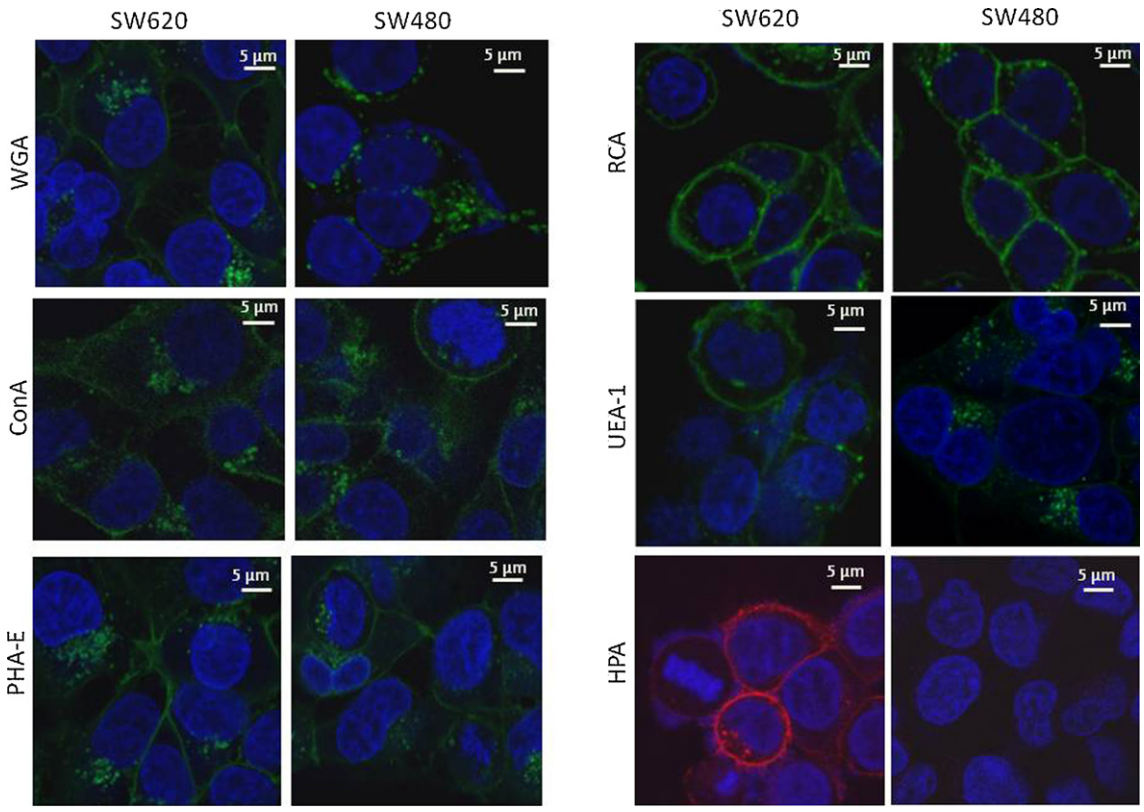

Fig. 3. Lectin binding to SW620 and SW480 cells as viewed using a Leica TCS SP2 confocal microscope. Cells were incubated with FITC labelled lectins WGA, RCA, ConA, PHA, RCA and UEA-1 (green) or TRITC labelled HPA (red), at 0.0632 mM for 1 h. The nuclei were counterstained with 1 mM To-Pro3 (blue). A 488 nm laser, was used for excitation of FITC, the emitted light was recorded over a bandwidth of 500–550 nm. A 543 nm laser was used for TRITC excitation and the emitted light was recorded over a bandwidth of 553–630 nm. A 633 nm laser was used for To-Pro-3 excitation with the emitted light recorded over a bandwidth of 650–720 nm. The images from the green/red channels were overlaid with the blue channel using the Imaris software system, version 7 (Bitplane). (For interpretation of the references to colour in this figure legend, the reader is referred to the web version of this article.)

3.1. Comparison of native and recombinant HPA binding to SW620 and SW480 cells

The preparation of recombinant proteins as reagents for diagnostic and therapeutic applications is an area of considerable activity (Pavlou and Reichert, 2004). The lectin HPA, from the Roman snail, *H. pomatia*, is of some interest as it has been shown to bind metastatic breast, colorectal and other cancers (Leathem and Brooks, 1987; Schumacher and Adam, 1997). We have produced recombinant HPA and are assessing its use as a reagent for discriminating between aggressive and non-aggressive epithelial cancers (Markiv et al., 2011). Recombinant proteins prepared with reporter proteins attached, for example, green fluorescent protein, GFP and red fluorescent protein, RFP, have found widespread application in cancer research but there has been concern that these reporter proteins may interfere with relatively low affinity interactions (for example those between lectins and their glycan ligands). In this study, the binding of native HPA (purchased from Sigma, UK), His-tagged HPA and RFP-tagged HPA was evaluated. The relative size of RFP was compared with the lectin HPA *in silico* using SwissModel, Supplementary data 2. From the Swiss-Model analysis RFP was observed to be bulky enough to, potentially, occlude the binding site of the HPA and we were interested in determining if the attachment of this tag affected the affinity of lectin–cell interactions. First the binding of native HPA to metastatic, SW620, and non-metastatic, SW480, cells was compared. Between each sensor experiment the cells were regenerated. The cells were re-probed with the appropriate lectin and observed to show the same frequency shift on application of lectin following regeneration, illustrating that the regeneration step does not alter the subsequent lectin binding properties. In addition, the detector response was monitored and observed to return to the same level as prior to the initial lectin analysis. The affinity (dissociation constant, K_D) of HPA to metastatic SW620 cells was in the nanomolar range, however, to the non-metastatic cells, SW480, the K_D values were in the micromolar range, Table 1. This is the first time, to our knowledge, that differences in reactivity of HPA to cancer cells has been correlated with the lectin affinity at the cell surface, and the differences appear to result from a reduced association rate constant (k_{on}) of HPA to the non-metastatic cells, SW480.

The interaction between native HPA and the metastatic SW620 cancer cell surfaces was compared with lectin binding to glycoproteins (from the same passage of cells) immobilised on the polystyrene biosensor chip, Fig. 2. This enabled a direct comparison between the binding of HPA to the intact cell surface and the affect of affinity measurements when glycoproteins are immobilised on the chip surface. The affinity of the lectin to the SW620 cell surface was greater than to glycoproteins; K_D, for HPA from the surface of SW620 cells 118 nM, and K_D from glycoproteins immobilised on chip, 859 nM. Similarly, the dissociation constant, K_D, for the recombinant HPA to SW620 cells grown on the biosensor chip surface and proteins was determined, Fig. 2. Consistent with the native material, the recombinant HPA bound cells in a concentration dependent manner (sensorgrams for HPA-His shown, Fig. 2). Both forms of recombinant HPA also showed greater affinity to the cells than native HPA (K_D HPA-His = 8.84 nM; HPA-RFP = 7.18 nM; native HPA = 118 nM) indicating a tighter binding of recombinant HPA to the cell surface. The difference in the K_D between native HPA and recombinant HPA appears to be due to a comparatively

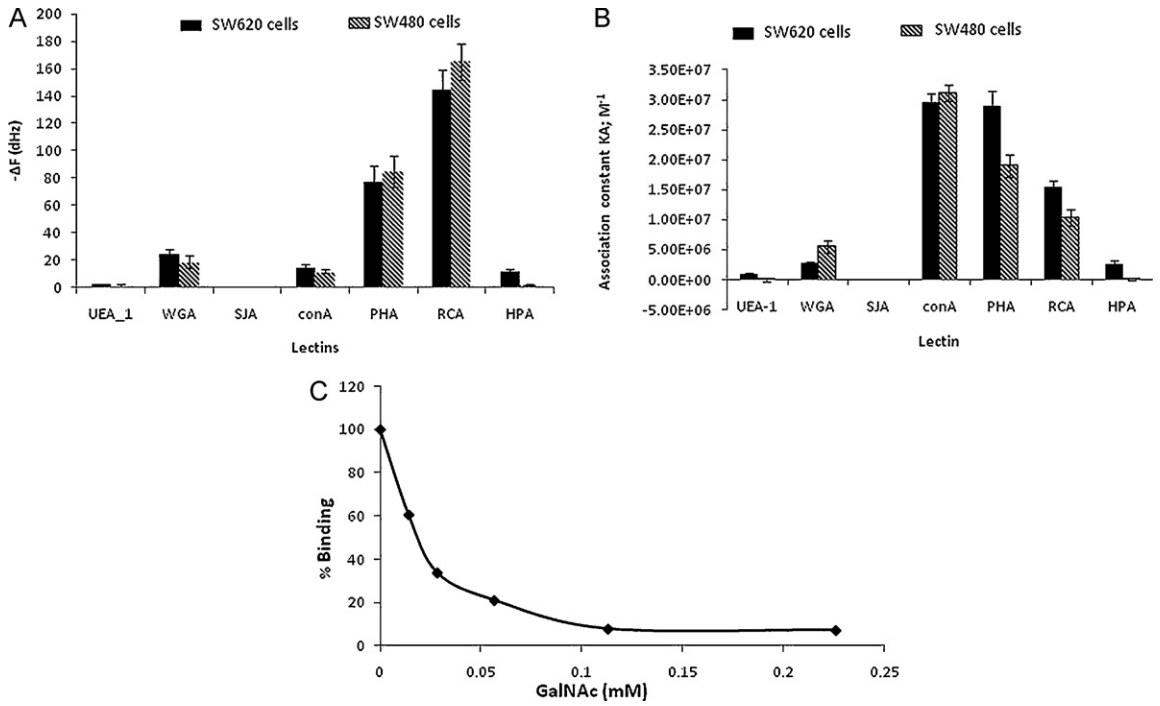

Fig. 4. Evaluation of lectin binding to SW620 and SW480 cells. The mean average values ± SD are shown for the association rate constant and the shift in the QCM frequency ($-\Delta F$) for UEA-1, WGA, SJA, ConA, PHA-E, RCA, and HPA with SW620 and SW480 cells (Panels A and B). The lectins RCA and PHA bound tightly to both SW620 and SW480 cells whilst UEA-1, WGA, SJA, ConA and HPA showed much weaker binding (Panel A). When the lectin binding was assessed in terms of the association constant (k_{on}), the pattern differed again (panel B), ConA had previously been observed to bind weakly to both SW620 and SW480 but the k_{on} was the greatest of all the lectins, conversely, RCA had previously been observed to give the highest $-\Delta F$ values but the k_{on} was lower than either ConA or PHA. Panel C: GalNAc dependent inhibition of HPA binding to SW620 cells was assessed by pre-incubation of HPA with 0.01–23 mM GalNAc for 30 min. Appropriate concentrations of GalNAc were used as the reference injection values. The maximal frequency shift monitored at the end of the association phase (after referencing with the GalNAc-containing solution) was used to calculate the percentage binding taking non-treated HPA as 100%.

low dissociation rate constant for the His-tagged and RFP-tagged proteins from the cell surface (Fig. 2).

We previously reported glycan-array analysis in which native HPA recognised many glycosylated epitopes whilst HPA-His bound fewer glycans, specifically those terminating in α-GalNAc (Markiv et al., 2011). Further, work with the simple epitope GalNAc-BSA and surface plasmon resonance analysis showed that recombinant HPA bound to GalNAc-BSA with greater affinity than native HPA (Markiv et al., 2011). From this we infer that the recombinant material would be expected to bind to fewer epitopes at the cell surface than native HPA but at a higher affinity, in particular those epitopes terminating in α-GalNAc.

Both His-tagged and RFP-tagged HPA had a similar affinity for the SW620 cells. This experiment demonstrated that the linker of 30 amino acids between the HPA and RFP proteins is long enough to prevent stearic hindrance of the glycan binding sites (Supplementary data 2). An attempt to determine dissociation rate constants by microtitre plate assay proved unsuccessful (data not shown) due to the very rapid binding of HPA to the cell surface in the microtitre plate environment, again emphasising the utility of the QCM technology for measuring lectin: cell interactions in real time.

3.2. Kinetic parameters of lectin–cell surface interactions

The kinetics of lectin–cell interactions was determined for a variety of lectins using the SW620 and SW480 cells. The binding rate constant (k_{on}) as well as the dissociation constant (K_D) varied according to the lectin and the cell type (SW620 or SW480) studied, Table 1. The dissociation constant, K_D, for the majority of the lectins to the cell surfaces was in the nanomolar range. The values measured for the affinity of PHA (K_D = 34.4 nM) to SW620 cells was in good agreement with the dissociation constant, K_D, reported when isolated mouse intestinal epithelial cells were studied using a different methodological approach (K_D = 66.7 nM) (Donatucci et al., 1987). The interaction between the lectins HPA and UEA-1, to SW480 cells was, however, 1/1000 to 1/10,000 fold weaker than for the other lectins studied (K_D: 980 μM and 23.7 μM, respectively) and was consistent with an observed reduction in the association rate constant, k_{on}, for HPA and UEA-1 to SW480 cells.

When the cells were incubated with fluorescently labelled lectin and viewed using the confocal microscope, Fig. 3, the binding patterns correlated with the values for the affinity measurements obtained with the cell biosensor. For example, SW620 cells were observed to bind HPA intensely at both the membrane surface and in the cytoplasm, whilst SW480 cells showed very minimal staining, agreeing with the values determined in the biosensor work, see above. The higher affinity of UEA-1 to SW620 cells in comparison to SW480 cells indicates an elevation in fucosylation in the metastatic cancer cells. However, the association rate constant (k_{on}) varied considerably according to both lectin and the cells tested, Table 1 and Fig. 4, so, whilst the lectin binding pattern (as measured by cytochemical staining and K_D values) appeared similar, the cell biosensor enabled subtle differences in the rate of binding to be measured and that this varied according to both the cell type and the lectin studied.

3.3. Inhibition HPA binding to SW620 by GalNAc

When HPA was pre-incubated with freshly prepared GalNAc and injected over the biosensor chip a dose dependent inhibition of HPA binding was observed (Fig. 4) thereby illustrating the specificity of lectin binding to carbohydrate residues (Hammarstrom and Kabat, 1971).

3.4. Comparison of lectin–cell interactions with previous studies

The results obtained in this study were compared with affinity data for lectin–carbohydrate interactions reported previously (Barnes et al., 1992; Duverger et al., 2003; Markiv et al., 2011; Pedroso et al., 2008). The interaction between a lectin and its glycan ligand is complicated by many factors, for example, the valency of the lectin, the branching of the carbohydrate structures, avidity and the nature of the immobilised partner (Duverger et al., 2003). One or more of these factors may explain some of the apparent discrepancies between the data reported in the literature. A study investigating the interaction between the lectin WGA and chitooligosaccharide, reported a value for the dissociation constant, of 58.8 μM when WGA was immobilised on the chip surface but a significantly different value of 5.88 nM when the polysaccharide was immobilised, showing that the affinity values measured are dramatically affected depending on which of the partners were immobilised on the chip surface (Shinohara et al., 1997). Similarly the K_D for the interaction between HPA and GalNAc differed six fold depending on the nature of the immobilised binding partner, *i.e.* K_D = 758 nM when GalNAc was immobilised (Markiv et al., 2011) whilst the K_D was 1.2 mM when HPA was immobilised. Studies addressing lectin–carbohydrate interactions normally involve measurements where the lectin binding is assessed to single well-defined glycan epitopes, but cells display a complex mixture of epitopes, making it exceedingly difficult to compare the results from these different systems.

We have measured the interaction between formalin-fixed cells and a range of lectins and report here diverse on-rates and K_D values compared with conventional systems in which ligands are attached to planar surfaces, for example in conventional QCM and SPR based systems. Although the fluidity that is a normal feature of cell membranes will undoubtedly be compromised during the cellular fixation process, none-the-less, this new cell-system offers distinct advantages over the more set-up that is represented in existing biosensors. The differences that we observed between the lectin interaction at the cell surface and immobilised proteins illustrates the importance of studying the binding properties of lectins (and other biomolecules) using intact cells.

4. Conclusions

This new biosensor allows quantitative evaluation of molecular interactions in a much more relevant cellular environment compared with conventional systems which utilise immobilised proteins (for example receptors) on the chip surface. The results provide a new insight into lectin–carbohydrate interactions at the cell surface while the binding data for the interaction between lectins and immobilised proteins correlated with previous well-established methods such as SPR. This methodology will be of interest to researchers working in diverse fields, focussing on biological approaches towards targeting cell surfaces in diseased tissues, or in understanding biological interactions at the cell surface. Future studies will be concerned with using living cells as the next step towards understanding the dynamics of molecular interactions at the cell surface.

Acknowledgements

DP acknowledges receipt of funding from Against Breast Cancer (Registered Charity Number 1121258). AM thanks Professor Ray St. Ledger, University of Maryland, for providing the mRFP1 DNA. We thank Dr Marilena Loizidou, University College London for the SW480 and SW620 cells.

Appendix A. Supplementary data

Supplementary data associated with this article can be found, in the online version, at doi:10.1016/j.bios.2012.02.037.

References

Barnes, C., d'Silva, C., Jones, J.P., Lewis, T.J., 1992. Sens. Actuators B 7, 347–350.
Brooks, S.A., Dwek, M.V., Leathem, A.J., 1998. Histochem. J. 30, 609–615.
Cooper, M.A., Singleton, V.T., 2007. J. Mol. Recognit. 20, 154–184.
Donatucci, D.A., Liener, I.E., Gross, C.J., 1987. J. Nutr. 117, 2154–2160.
D'Ulivo, L., Saint-Guirons, J., Ingemarsson, B., Riekkola, M., 2010. Anal. Bioanal. Chem. 396, 1373–1380.
Duverger, E., Frison, N., Roche, A., Monsigny, M., 2003. Biochimie 85, 167–179.
Fredriksson, C., Kihlman, S., Rodahl, M., Kasemo, B., 1998. Langmuir 14, 248–251.
Hammarstrom, S., Kabat, E., 1971. Biochemistry 10, 1684–1692.
Johansson, T., 2010. In: Kontermann, R., Dübel, S. (Eds.), Antibody Engineering. Springer-Verlag, Berlin, Heidelberg, pp. 683–693.
Kuo, Y.-C., Ho, J.H., Yen, T.-J., Chen, H.-F., Lee, O.K.-S., 2011. PLoS ONE 6 (7), e22382, doi:10.1371/journal.pone.00223827.
Leathem, A.J., Brooks, S.A., 1987. Lancet 329, 1054–1056.
Lehner, I., Niehof, M., Borlak, J., 2003. Electrophoresis 24, 1795–1808.
Markiv, A., Peiris, D., Curley, P., Odell, M., Dwek, M.V., 2011. J. Biol. Chem. 286, 20260–20266.
Marx, S., Kaushansky, N., Gratziany, N., Barness, I., Liron, Z., 2001. Biosens. Bioelectron. 16, 239–244.
Marx, K.A., 2003. Biomacromolecules 4, 1099–1120.
Modin, C., Stranne, A.L., Foss, M., Duch, M., Justesen, J., Chevallier, J., Andersen, L.K., Hemmersam, A.G., Pedersen, F.S., Besenbacher, F., 2006. Biomaterials 27, 1346–1354.
Nirmalan, N.J., Harnden, P., Selby, P.J., Banks, R.E., 2008. Mol. Biosyst. 4, 712–720.
Pavlou, A.K., Reichert, J.M., 2004. Nat. Biotechnol. 22, 1513–1519.
Pedroso, M.M., Watanabe, A.M., Barreira, M.C.R., Bueno, P.R., Faria, R.C., 2008. Microchem. J. 89, 153–158.
Pei, Z., Anderson, H., Aastrup, T., Ramstrom, O., 2005. Biosens. Bioelectron. 21, 60–66.
Saint-Guirons, J., Zeqiraj, E., Schumacher, U., Greenwell, P., Dwek, M., 2007. Proteomics 7, 4802–4809.
Saitakis, M., Dellaporta, A., Gizeli, E., 2008. Biophys. J. 95, 4963–4971.
Saitakis, M., Gizeli, E., 2012. Cell. Mol. Life Sci. 69, 357–371.
Sauerbrey, G., 1959. Z. Phys. 155, 206–222.
Sanchez, J.F., Lescar, J., Chazalet, V., Audfray, A., Gagnon, J., Alvarez, R., Breton, C., Imberty, A., Mitchell, E.P., 2006. J. Biol. Chem. 2811, 20171–20180.
Schwede, T., Kopp, J., Guex, N., Peitsch, M.C., 2003. Nucleic Acids Res. 31, 3381–3385.
Schumacher, U., Adam, E., Zangemeister-Wittke, U., Gossrau, R., 1996. Acta Histochem. 98, 381–387.
Schumacher, U., Adam, E., 1997. Histochem. J. 29, 677–684.
Safina, G., Duran, I.B., Alasel, M., Danielsson, B., 2011. Talanta 84, 1284–1290.
Shinohara, Y., Hasegawa, Y., Kaku, H., Shibuya, N., 1997. Glycobiology 7, 1201–1208.
Yakovleva, M.E., Safina, G.R., Danielsson, B., 2010. Anal. Chim. Acta 668, 80–85.